

The ESR Spectra, Electronic Structure, and Thermal Reactivity of Fluoroethane Cations

Kenji Komaguchi, Hiroshi Sakurai, Masaru Shiotani, and Akinori Hasegawa[*,†]

Department of Applied Chemistry, Graduate School of Engineering, Hiroshima University, Higashi-Hiroshima 739-0046

†Department of Chemistry, Kogakkan University, Ise-shi 516-8555

(Received June 25, 2001)

The ESR spectra for the cation radicals of CH_3CH_2F (FE) and its partially deuterated derivatives, formed by irradiation with γ-rays in SF_6 matrices at 77 K, were observed at low temperatures. The spectra consist of two lines typical of an anisotropic hyperfine coupling to a ^{19}F nucleus. The optimized geometry of $FE^{\bullet+}$ was obtained by the ab initio MO method, and hyperfine splittings were evaluated by density functional theory (DFT). Two structures, A and B, were obtained having $^2A'$ and $^2A''$ electronic states, respectively. Structure A is in a lower energy state by 0.31 eV than structure B, and is assigned to the detected cation radical. This structure has a SOMO composed of the 2p orbitals of two C and an F atoms in the molecular plane, and has an elongated C–C bond of 0.1884 nm. This resembles the SOMO given for $C_2H_6^{\bullet+}$. Furthermore, the structural distortion of $FE^{\bullet+}$ in zeolite and the thermal dissociation of $FE^{\bullet+}$ in matrices are reported.

A number of studies have been reported on the electronic structures for the cation radicals of the hydrocarbons substituted by halogens, since substitution by halogens can induce large effects in the geometric and electronic structure of organic molecules.[1–6] For example, the ethylene cation and the propene cation have nonplanar twisted structures,[7,8] while the fluorinated ethylene and propene cations were concluded to have planar structures.[5]

Iwasaki et al. reported that the ESR spectrum of $C_2H_6^{\bullet+}$ consisted of three lines with binominal 1:2:1 intensities and that the unpaired electron possessed a $4a_g$ orbital in a C_{2h} symmetry.[9] This is a cation of the σ-type; a spin density of ca. 60% lies in the 1s orbitals of the two hydrogen atoms in the plane of the molecule (Scheme 1). On the other hand, Knight et al. observed the ESR spectrum of $CH_3F^{\bullet+}$ trapped in a Ne matrix.[10] In this cation of the π-type, ca. 24% of the unpaired electron is occupied in a 2p orbital of ^{19}F and ca. 67% in the 1s orbitals of the three hydrogen atoms (Scheme 1).

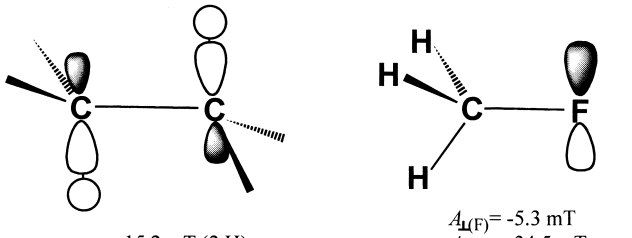

$a_{(H)}$=15.2 mT (2 H)

$A_{\perp(F)}$= -5.3 mT
$A_{/\!/(F)}$= -34.5 mT
$a_{(H)}$=11.3 mT (3 H)

$CH_3CH_3^{\cdot+}$ [8,9] $CH_3F^{\cdot+}$ [10]

Scheme 1.

In this study, the electronic structure of the cation radical of fluoroethane ($FE^{\bullet+}$) was investigated. $FE^{\bullet+}$ can be thought to be a radical yielded by the substitution of a hydrogen atom in the $C_2H_6^{\bullet+}$ radical of the σ-type by a fluorine atom. Therefore, a study of the electronic structure of $CH_3CH_2F^{\bullet+}$ may provide fundamental experimental information on the substitution effects of *n*-alkanes by fluorine atoms. On the other hand, $FE^{\bullet+}$ can also be compared to the radical produced by the substitution of a hydrogen atom in the $CH_3F^{\bullet+}$ radical of the π-type by a CH_3 group. Accordingly, the electronic structure and the distribution of the spin density for $FE^{\bullet+}$ were investigated by ESR measurements and molecular-orbital calculations, and were compared with those of $C_2H_6^{\bullet+}$ and $CH_3F^{\bullet+}$. The thermal reaction of $FE^{\bullet+}$ was also studied by the ESR method, and the reactivity of $FE^{\bullet+}$ is discussed. Moreover, the surface effect for $FE^{\bullet+}$ adsorbed on zeolite is considered.

Experimental and Calculations

CH_3CH_2F (FE) and its two partially deuterated derivatives, CH_2DCH_2F and CD_3CH_2F, were used as solutes. CH_3CH_2F (97%) was purchased from Takachiho Co. Ltd. and CH_2DCH_2F and CD_3CH_2F were supplied by Professor Emeritus Michiro Hayashi of the Faculty of Science, Hiroshima University. SF_6 (Takachiho Co. Ltd.) and Na-ZSM5 zeolite (SiO_2/Al_2O_3 = 23.8, TOSOH Co. Ltd.) were used as matrices. Solutions containing about 1 mol% of FE in matrices were prepared in Spectrosil ESR sample tubes on a vacuum line. For the experiments using zeolite, 10 wt% FE was introduced and adsorbed at room temperature on zeolite, which had been subjected to a thermal treatment at 200 °C for 2 hours in air followed by a treatment at 400 °C for 4 hours under a vacuum. The samples were irradiated with γ-rays from a ^{60}Co source at 77 K, the typical total absorption dose being about 10 kGy. ESR measurements were conducted with a Bruker ESP300E spectrometer operating at a 100 kHz field modulation of 0.32 mT

and a microwave power of 1.0 mW, in the temperature region of 4 K to 150 K.

The optimized geometry of $FE^{\bullet+}$ was obtained by the ab initio MO method at the MP2/6-31G** level, and isotopic and anisotropic hyperfine splittings were evaluated for the structure by the density functional theory (DFT) at the B3LYP/6-31G** level.[11] All calculations were carried out on a Dell Precision 410 workstation using the GAUSSIAN 98 program package.

Results and Discussion

ESR of Fluoroethane Cations in SF_6 Matrices. The ESR spectrum observed from an irradiated SF_6 matrix containing CH_3CH_2F at 77 K, consists of two anisotropic lines typical of the hyperfine splitting due to a ^{19}F nucleus, as shown in Fig. 1a. No obvious change in the spectrum was observed in the rage of 4 to 95 K, but, by annealing to higher temperatures, the spectrum changed reversibly into an isotropic spectrum. In the spectrum observed at 100 K, two different radicals, ((I) and (II)) having the following parameters, were found in addition to $SF_6^{\bullet-}$ and $SF_5^{\bullet}$ radicals,[12,13] as described in a below section:

(I) 2.2 mT ($2 \times {}^1H$) and 2.6 mT ($3 \times {}^1H$),

(II) 6.8 mT ($1 \times {}^{19}F$), 2.2 mT ($1 \times {}^1H$), and 2.5 mT ($3 \times {}^1H$).

Radicals (I) and (II) were assigned to $CH_3CH_2^{\bullet}$ [14] and $CH_3CHF^{\bullet}$,[15] respectively, based on these ESR parameters. Thus, the radical, strongly suggested as the $FE^{\bullet+}$ cation and giving the spectrum in Fig. 1, may be a precursor for neutral radicals (I) and (II).

The ESR spectra of $CH_2DCH_2F^{\bullet+}$ and $CD_3CH_2F^{\bullet+}$, generated in SF_6 matrices and observed at 77 K, are slightly different in their line-widths, but are essentially the same as the spectrum of $CH_3CH_2F^{\bullet+}$, as shown in Fig. 1. Thus, since partially deuterated samples gave no change in the hyperfine splitting (hfs), it may be concluded that the hfs of the ^1H in the CH_3 group is smaller than the line-width (0.5 mT).

The ESR spectrum of $CH_3CH_2F^{\bullet+}$ was reproduced by a simulation using the ESR parameters of $A_{//}(^{19}F) = 13.0$ mT, $A_{\perp}(^{19}F) = 0.5$ mT, $a(2 \times {}^1H) = 0.9$ mT, $a(3 \times {}^1H) < 0.5$ mT, $g_{xx} = 2.0053$, $g_{yy} = 2.0072$, and $g_{zz} = 2.0054$, as shown in Fig. 1. From the isotropic hfs of $a(2 \times {}^1H) = 0.9$ mT, ca. 4% of the unpaired electron is found to be occupied in the two 1s orbitals of the equivalent ^1H atoms.

Since the observed ^{19}F hf tensor can be assumed to be uniaxially symmetric, isotropic $a(^{19}F)$ and anisotropic $b(^{19}F)$ hf tensors can be obtained in terms of the observed $A_{//}(^{19}F)$ and $A_{\perp}(^{19}F)$ from the following equations:[16]

$$A_{//}(^{19}F) = a(^{19}F) + 2b(^{19}F),$$

$$A_{\perp}(^{19}F) = a(^{19}F) - b(^{19}F).$$

Although the sign of $A_{\perp}(^{19}F)$ could not be determined from ESR measurements, the value $A_{\perp}(^{19}F)$ is much smaller than that of $A_{//}(^{19}F)$. Thus, the value of $b(^{19}F)$ is only slightly affected by the sign of $A_{\perp}(^{19}F)$, since the value is 4.2 and 4.5 mT for the positive and negative signs, respectively, of $A_{\perp}(^{19}F)$. It is concluded from the atomic anisotropy of 54.3 mT[17] for ^{19}F that ca. 8% of the unpaired electron is localized in a 2p orbital of the ^{19}F atom.

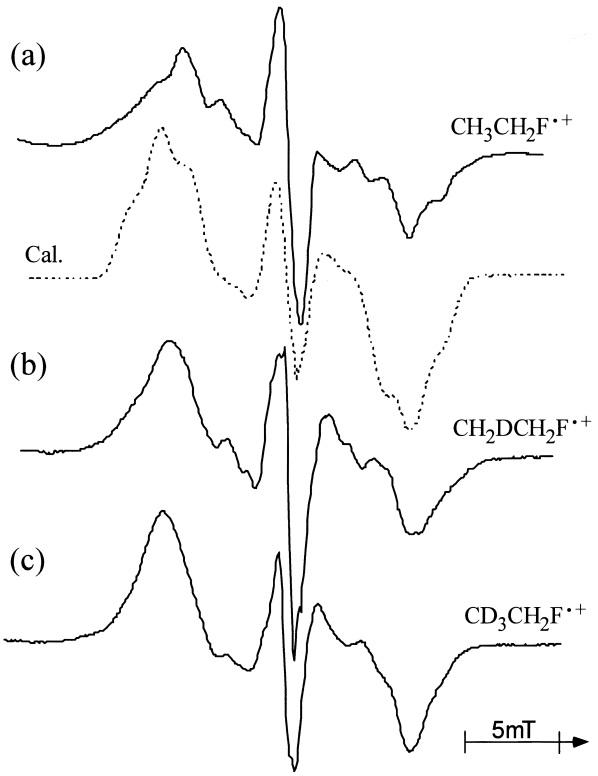

Fig. 1. ESR spectra of (a) $CH_3CH_2F^{\bullet+}$, (b) $CH_2DCH_2F^{\bullet+}$, and (c) $CD_3CH_2F^{\bullet+}$ formed in SF_6 matrices by ionizing radiation, and recorded at 77 K. The dotted lines are the simulation spectrum calculated using the following ESR parameters: $A_{//}(^{19}F) = 13.0$ mT, $A_{\perp}(^{19}F) = 0.5$ mT, $a(^1H$ in $CH_2F) = 0.9$ mT, $a(^1H$ in $CH_3) < 0.5$ mT, $g_{xx} = 2.0053$, $g_{yy} = 2.0072$, and $g_{zz} = 2.0054$. The Gaussian line shape with a line-width of 0.5 mT was used.

ESR of Fluoroethane Cations Adsorbed on Zeolites. The ESR spectra of the $CH_3CH_2F^{\bullet+}$ and $CH_2DCH_2F^{\bullet+}$ cations generated in the matrices of Na-ZSM5 zeolite are shown in Figs. 2a and b, respectively. For a comparison, the spectrum of $CD_3CH_2F^{\bullet+}$ in SF_6 is also shown in Fig. 2c. The $A_{//}(^{19}F)$ value of $FE^{\bullet+}$ in the zeolite is larger by ca. 3 mT than that in SF_6. This difference may result from the fact that the geometric structure of the cations is affected by adsorption on crystalline zeolite, having a 0.5 nm size channel.[18–21]

MO Calculation Results. $CH_3CH_2F^{\bullet+}/SF_6$ System. Ab initio MO calculations were conducted to elucidate the electronic structure of $CH_3CH_2F^{\bullet+}$ in more detail. Two different optimized geometric structures, A and B, were obtained by using the GAUSSIAN 98 program at the MP2/6-31G** level, as shown in Fig. 3. The total energy for structure A with the $^2A'$ electronic state (C_s structure) of the σ-type is lower by ca. 0.31 eV than that of structure B in the $^2A''$ electronic state (C_s structure) of the π-type, as shown in Fig. 3. The theoretical values of not only isotropic but also anisortopic ^{19}F- and ^1H-hfs for these two structures were evaluated by DFT method at the B3LYP/6-31G** level.[11] The calculated hf tensors and the di-

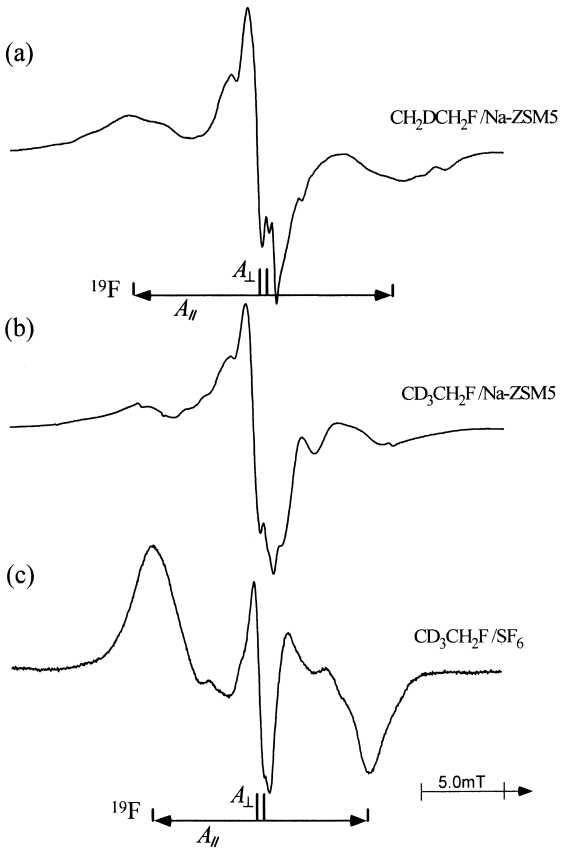

Fig. 2. ESR spectra of (a) $CH_2DCH_2F^{\bullet+}$ and (b) $CD_3CH_2F^{\bullet+}$ generated in Na-ZSM5 zeolite matrices by ionizing radiation, and recorded at 77 K. Spectrum (C) is for $CD_3CH_2F^{\bullet+}$ generated in an SF_6 matrix (Fig. 1c).

rections for the ^{19}F nucleus and isotropic couplings to ^1H nuclei are shown with the observed values in Figs. 3a and b.

The SOMO of structure A is mainly composed of the 2p orbitals, of the two C and the F atoms, which are in the molecular plane, whereas that for the structure B is done with the 2p orbitals perpendicular to the molecular plane. The difference in the two electronic states results in a large difference in the C–C bond lengths. The C–C bond length of structure A is 0.1884 nm, elongated by ca. 25% from 0.1509 nm for its neutral molecule (Fig. 4), while that of structure B is 0.1458 nm, reduced only by ca. 3.3%.

Regarding the hfs to the ^{19}F nucleus of structure A, the calculated $A_{//}$ value, 31.5 mT, is ca. 2.4-times larger than the observed one, 13 mT, and the calculated $A_\perp$, (−)7.3 mT, is ca. 15-times larger than the observed one, ca. 0.5 mT. The calculated isotropic hfs of the two ^1H nuclei in the CH_2F group, 1.4 mT, is close to the observed one, 0.9 mT, and the value averaged among the three ^1H nuclei in the CH_3 group, −0.15 mT, is consistent with the observed one, < 0.5 mT. On the other hand, for structure B, not only the reproduction of the hfs to ^{19}F is unsatisfactory, but also the isotropic coupling for the ^1H nuclei in the CH_2F group is 18-times larger than the observed value. Thus, structure A might be reasonably assigned to the cation generated, if it is taken into consideration that a small difference in the calculated unpaired electron density gives rise to a large difference in hfs for the ^{19}F nucleus because of the large value of the magnetic moment of the nucleus.

To the best of our knowledge, a few DFT calculations have been carried out for such radical species containing F atoms as $F_2^{\bullet-}$,[22] $FCl^{\bullet-}$,[22] $F^\bullet$,[23,24] and $FOO^\bullet$,[25] but there is no report for cation radicals containing F atoms. As a matter of course, the fitting between the calculated and observed hfs for these four species reported is unsatisfactory, since the hfs values for ^{19}F is largely dependent upon its spin density.

In order to compare the electronic structure between $FE^{\bullet+}$ and $C_2H_6^{\bullet+}$, the optimized structure of $C_2H_6^{\bullet+}$ was evaluated at the MP2/6-31G** level and two electronic states, ^2A_g and ^2B_g (C_{2h}), were obtained. The ^2A_g state is a σ-type and the ^2B_g state is a π-type, having C–C bond lengths of 0.1584 nm and 0.1435 nm, respectively, as shown in Fig. 3. They are elongated and shortened as compared with that of the neutral CH_3CH_3 molecule, 0.1542 nm. The ^2A_g state is in a lower energy state by ca. 0.2 eV, in accord with the results reported by Iwasaki et al.[8,9] Structure A for $FE^{\bullet+}$ in the $^2A'$ is analogous to the ^2A_g state of $CH_3CH_3^{\bullet+}$, while the B structure corresponds to the ^2B_g state. Thus, the substitution of one H atom in the $CH_3CH_3^{\bullet+}$ cation by an F atom is ineffective with regard to the electronic ground state, and the electronic state similar to the ^2A_g state is retained, although the unpaired electron density is partly distributed on the F atom. The meta stable structure B, in a π-type, corresponds to the structure assigned to $CH_2F^{\bullet+}$.[10]

Optimized geometries for neutral mother molecules of C_2H_5F and C_2H_6, shown in Fig. 4, were compared with those of these cation radicals. Structure A for $FE^{\bullet+}$ is formed by elongating the C–C bond with a σ bonding nature and shortening the C–F bond with a π antibonding nature, whereas structure B has shortened C–C and C–F bonds both with a π antibonding nature. Similar behavior was obtained for the C–C bonds in the ^2A_g and ^2B_g states for $CH_3CH_3^{\bullet+}$.

This trend is in agreement with that which we have concluded in our recent study on the cation radicals of fluorinated benzenes.[6] It depends upon the process of releasing one electron from an HOMO; the chemical bonds with the bonding nature in the HOMO become elongated and that the bonds with an antibonding nature become shortened.

Hfs values of 0.9 mT to < 0.5 mT are given to the ^1H nucleus in $FE^{\bullet+}$, and are too much smaller than 15.2 mT for two ^1H nuclei in the molecular plane of $C_2H_6^{\bullet+}$ [8,9] and 11.3 mT for three ^1H nuclei in the $CH_3F^{\bullet+}$.[10] The large amount of spin density, ca. 60%, is occupied by the two hydrogens in the case of $C_2H_6^{\bullet+}$, and ca. 67%, is possessed by the three hydrogens in $CH_3F^{\bullet+}$. However, the large spin density moves into the 2p orbitals of two C atoms in the case of $FE^{\bullet+}$.

When the cation radicals of a series of fluorinated ethylenes were compared, in the order of $CF_2{=}CH_2^{\bullet+}$, $CF_2{=}CFH^{\bullet+}$, $CF_2{=}CF_2^{\bullet+}$, the observed isotropic and anisotropic hfs to the ^{19}F nuclei in the CF_2 groups systematically increased with the number of F atoms in the group of the counterpart of the CF_2 group.[5] This phenomenon was interpreted in terms of the "back donation" effect of the fluorine, which has a high electronegativity and behaves as a π donor.[26] The concentration of the spin density to the 2p orbitals of two C atoms, which was brought about by substitution of $C_2H_6^{\bullet+}$ by a fluorine atom in this study, is also explained as the "back donation" effect of the

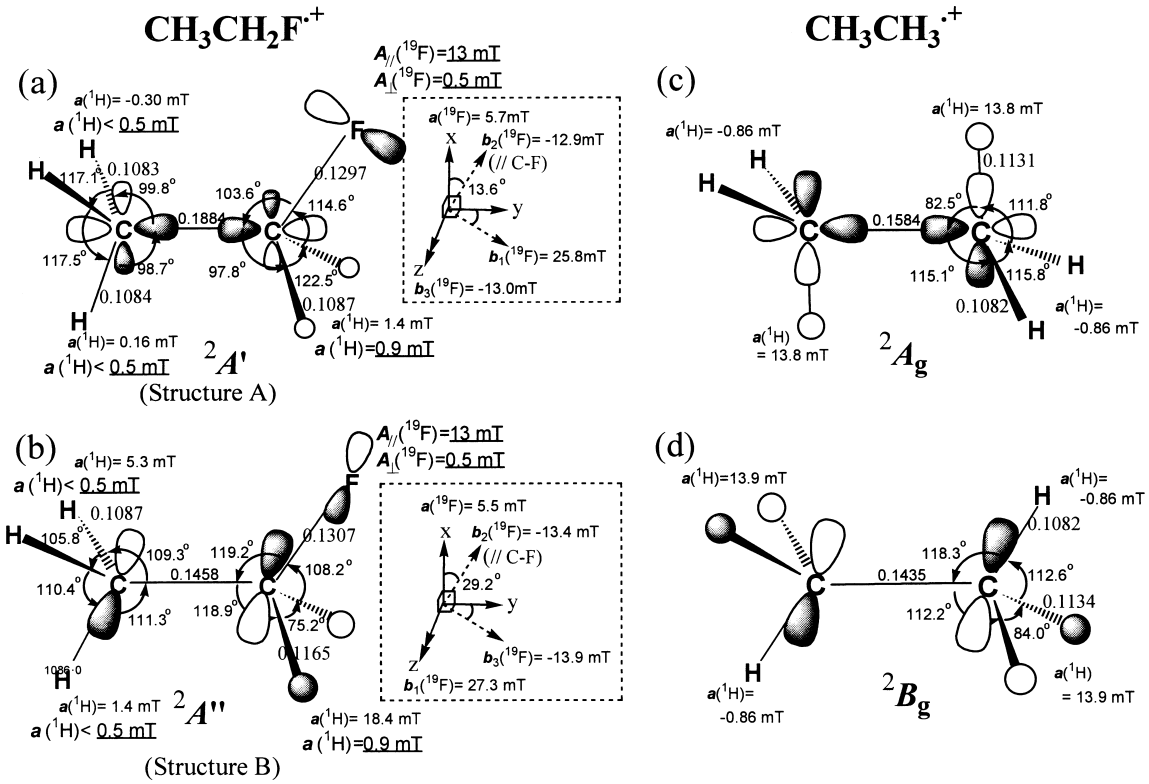

Fig. 3. Optimized geometries with the schematic representation of SOMOs for $CH_3CH_2F^{\bullet+}$ and $CH_3CH_3^{\bullet+}$ calculated using a GAUSSIAN 98 program at the MP2/6-31G** level, together with the ^{19}F-hf tensors and isotropic ^{1}H couplings calculated by DFT method at the level of B3LYP/6-31G**. The observed hf couplings to ^{1}H and ^{19}F nuclei are given with underlines. The bond lengths are in nm. The p orbitals contributing the SOMO in structure A are in the molecular plane, while those in structure B are perpendicular to the molecular plane.

fluorine.

The hfs of the methyl protons in $FE^{\bullet+}$ is negligibly small. Positive spin is caused by super conjugation from the C atom in the CH_2F group, but negative spin through a spin polarization from the methyl C atom. The sum of the positive and negative spin gives hfs to the methyl proton. This is one more reason why they have small hfs. The small hfs for methylene protons (0.9 mT) can be also explained using similar reasoning.

$CH_3CH_2F^{\bullet+}$/Na-ZSM5 System. The hf $A_{//}(^{19}F)$ tensor of the $FE^{\bullet+}$ generated in the zeolite is larger by ca. 3 mT than that formed in SF_6 matrices, as described above. This may result from the fact that the structure of the cation is subjected to some distortion through interactions between the cation and the zeolite surface. In order to attain any information on the structural deformation of $FE^{\bullet+}$ adsorbed on the zeolite, the DFT method at the level of B3LYP/6-31G** was used to calculate how the value of $A_{//}(^{19}F)$ and the total energy were changed when the C–C–F angle, θ, and the length of the C–F, r(C–F), and C–C, r(C–C), bonds were altered from those of the optimized geometry. The change in the values of $A_{//}$ and total energy, respectively, induced by change in θ and r is shown in Fig. 5.

The increased value in $A_{//}(^{19}F)$ of 3 mT, observed in the zeolite matrices, corresponds to ca. 23% of the observed value (13 mT) in SF_6 matrices. Since the optimized structure A has an $A_{//}(^{19}F)$ value of 31.5 mT, the value increased by 23% is ca. 38.8 mT. Thus, we searched for θ, r(C–F), and r(C–C), giving an $A_{//}(^{19}F)$ of 38.8 mT; $\theta = 87°$ and r(C–F) = 0.146 and r(C–C) = 0.169 nm were obtained. The structure having either parameter is in a higher energy state by ca. 0.0040 a.u (ca. 0.11 eV), 0.0190 a.u (ca. 0.52 eV) and 0.0046 a.u (ca. 0.13 eV) than the optimized one, respectively. Increase in $A_{//}$ value arisen in zeolite is possible for a structure with a smaller C–C–F bond angle, a longer C–F bond, and a shorter C–C bond. Although the deformation of the cation in zeolite cavity cannot be defined explicitly, elongation in the C–F bond, requiring a large increase in energy, may be difficult in the cavity, whereas the C–C bond shortened in the cavity may be plausible. A decrease in the C–C–F angle accompanied by the smallest increase in energy may also be possible.

Thermal Reactivity of Fluoroethane Cations. When $CH_3CH_2F^{\bullet+}$ generated in SF_6 was annealed to 100 K, where the matrix was in a plastic phase,[27] the spectra changed irreversibly. The spectrum observed at this temperature consisted of a number of complicated lines, making its analysis difficult. Thus, in order to identify the radical species formed, $CD_3CH_2F^{\bullet+}$ was annealed in place of $CH_3CH_2F^{\bullet+}$. The spectrum observed for $CD_3CH_2F^{\bullet+}$ at 100 K are shown in Fig. 6. A simulation indicates that in addition to the radicals of $SF_6^{\bullet-}$ and $SF_5^{\bullet}$, two kinds of radicals, III and IV, were generated in the ratio of 0.3:0.7, respectively, having the following ESR parameters:

(III) 2.2 mT (2 × ^{1}H) and 0.4 mT (3 × ^{2}D),

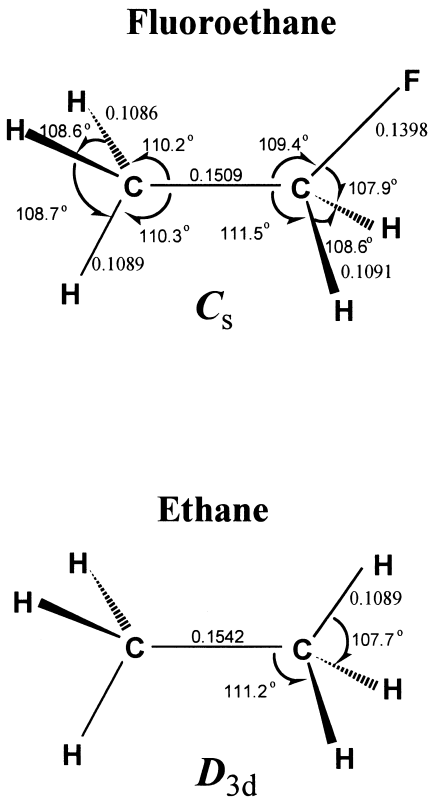

Fig. 4. Optimized geometries for the neutral molecules of CH_3CH_2F and CH_3CH_3, calculated with a GAUSSIAN 98 program at the MP2/6-31G** level to be compared with those of their radical cations.

(IV) 6.8 mT (1 × ^{19}F), 2.2 mT (1 × ^{1}H), and 0.4 mT (3 × ^{2}D).

From these parameters, radicals (III) and (IV) were assigned to $CD_3CH_2^{\bullet}$ and $CD_3CHF^{\bullet}$, respectively. Thus, the previous assignment to the neutral radicals $CH_3CH_2^{\bullet}$ and $CH_3CHF^{\bullet}$, giving the ESR parameters (I) and (II), was confirmed using a partially deuterated fluoroethane CD_3CH_2F. The complicated spectrum observed for $CH_3CH_2F^{\bullet+}$ at 100 K was successfully interpreted in terms of these assignments.

The followings are three possible reaction mechanisms for the radical formation:

$$\text{(a) } CH_3CH_2F^{\bullet+} \rightarrow CH_3CHF^{\bullet} + H^+ \quad (1)$$

$$H^+ + F^- \rightarrow HF \text{ or } H^+ + SF_6^{\bullet-} \rightarrow HF + SF_5^{\bullet} \quad (2)$$

$$\text{(b) } SF_6^{\bullet-} \rightarrow SF_5^{\bullet} + F^- \quad (3)$$

$$CH_3CH_2F^{\bullet+} + F^- \rightarrow CH_3CH_2^{\bullet} + F_2 \quad (4)$$

$$CH_3CH_2F^{\bullet+} + F^- \rightarrow CH_3CHF^{\bullet} + HF \quad (5)$$

$$\text{(c) } CH_3CH_2F^{\bullet+} + SF_6^{\bullet-} \rightarrow CH_3CH_2F^{*} + SF_6 \quad (6)$$

$$CH_3CH_2F^{*} \rightarrow CH_3CH_2^{\bullet} + F^{\bullet} \quad (7)$$

$$CH_3CH_2F^{*} \rightarrow CH_3CHF^{\bullet} + H^{\bullet} \quad (8)$$

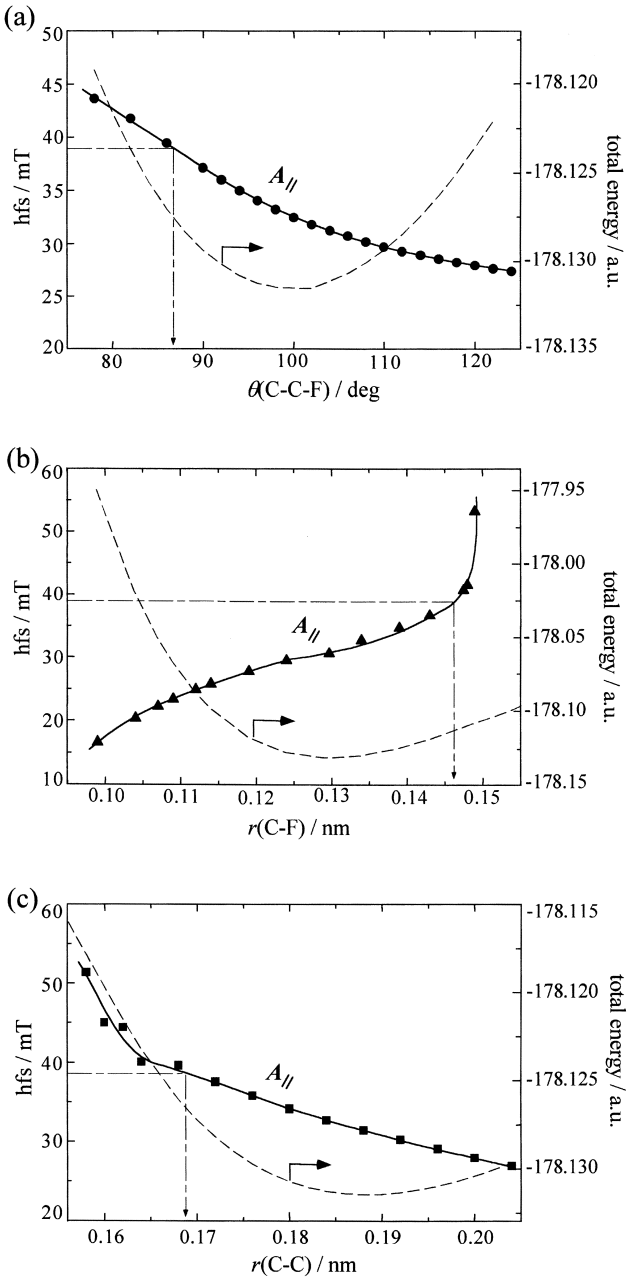

Fig. 5. The dependence of the $A_{//}$ coupling to the ^{19}F nucleus and the total energy on (a) the C–C–F angle, θ(C–C–F), and (b) the C–F, r(C–F), and (c) C–C bond, r(C–C), lengths calculated at the MP2/6-31G** level. The $A_{//}$ coupling was evaluated for each optimized structure using DFT method at B3LYP/6-31G** level.

The first mechanism (a) shows the neutral radical $CH_3CHF^{\bullet}$ formed by the removal of an H^+ from $FE^{\bullet+}$. This reaction may be followed by reaction (2). It may, however, be difficult to expect $CH_3CH_2^{\bullet}$ from a similar mechanism. The second mechanism (b) has the F^- released from $SF_6^{\bullet-}$ neutralizing $FE^{\bullet+}$ to form both the neutral radicals. The formation energies of H–F and F–F are 565.9 and 154.8 kJ mol^{-1}, respectively.[28] That is, the reaction to produce HF is thermodynamically more favorable than that to yield F_2. This might be somewhat related to the observed higher yield of $CH_3CHF^{\bullet}$ ($[CH_3CH_2^{\bullet}]$:$[CH_3CHF^{\bullet}]$ =

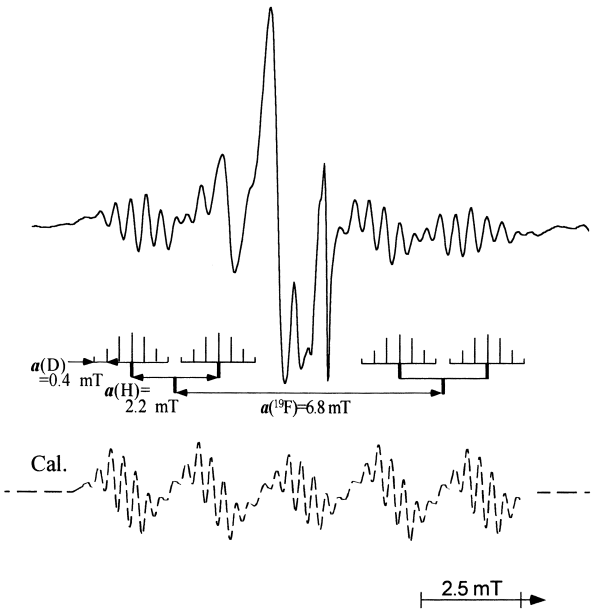

Fig. 6. ESR spectrum observed at 100 K for the CD_3CH_2F/SF_6 sample pre-irradiated at 77 K. The dashed line is a simulated spectrum by superposing the calculated spectra of $CD_3CH_2^{\bullet}$ and $CD_3CHF^{\bullet}$ with the relative ratios of 0.3 and 0.7, respectively. The parameters used for the simulation are given in the text.

3:7). The last mechanism (c) shows the neutral excited species of FE, FE^*, formed by the reaction between $FE^{\bullet+}$ and the electron released from $SF_6^{\bullet-}$ as a precursor to generate these neutral radicals. In this study, the ESR signals of these neutral radicals were observed with the appearance of the $SF_5^{\bullet}$ radical formed from $SF_6^{\bullet-}$. Therefore, mechanism (b) may be more plausible, although mechanism (a) is not completely ruled out.

This study was partially supported by grant from the Ministry of Education, Science, Sports and Culture. The authors thank Miss Nami Miwa for experimental assistance, Dr. Wang Pen for helpful discussions, and Professor Emeritus Michiro Hayashi for supplying partially deuterated fluoroethanes, CH_2DCH_2F and CD_3CH_2F.

References

1 A. Hasegawa, M. C. R. Symons, and M. Shiotani, *J. Chem. Soc., Perkin Trans. 2*, **1989**, 147.

2 A. Hasegawa, M. C. R. Symons, and M. Shiotani, *J. Chem. Soc., Perkin Trans. 2*, **1989**, 657.

3 M. Shiotani, H. Kawazoe, and J. Sohma, *J. Phys. Chem.*, **88**, 2220 (1984).

4 A. Hasegawa, M. Shiotani, and Y. Hama, *J. Phys. Chem.*, **98**, 1834 (1994).

5 Y. Itagaki, M. Shiotani, A. Hasegawa, and H. Kawazoe, *Bull. Chem. Soc. Jpn.*, **71**, 2547 (1998).

6 A. Hasegawa, Y. Itagaki, and M. Shiotani, *J. Chem. Soc., Perkin Trans. 2*, **1997**, 1625.

7 a) M. Shiotani, L. Sjöqvist, and A. Lund, unpublished data. b) S. Lunell and M. B. Huang, *Chem. Phys. Lett.*, **168**, 63 (1990).

8 K. Toriyama, K. Nunome, and M. Iwasaki, *J. Chem. Phys.*, **77**, 5891 (1982).

9 M. Iwasaki, K. Toriyama, and K. Nunome, *J. Am. Chem. Soc.*, **103**, 3591 (1981).

10 L. B. Knight, Jr., B. W. Gregory, D. W. Hill, C. A. Arrington, T. Momose, and T. Shida, *J. Chem. Phys.*, **94**, 67 (1991).

11 F. Fängström, S. Lunell, B. Engels, L. Eriksson, M. Shiotani, and K. Komaguchi, *J. Chem. Phys.*, **107**, 297 (1997).

12 R. W. Fessenden and R. H. Schuller, *J. Chem. Phys.*, **45**, 1845 (1966).

13 A. Hasegawa and F. Williams, *Chem. Phys. Lett.*, **45**, 275 (1977).

14 R. W. Fessenden, *J. Mag. Reson.*, **1**, 27 (1969).

15 K. S. Chen and J. K. Kochi, *J. Am. Chem. Soc.*, **96**, 794 (1974); K. S. Chen and J. K. Kochi, *Can. J. Chem.*, **52**, 3529 (1974).

16 M. Iwasaki, *Mol. Phys.*, **20**, 503 (1971).

17 B. A. Goodman and J. B. Raynor, *Adv. Inorg. Chem. Radiochem.*, **13**, 135 (1970).

18 J. Turkevich and Y. Fujita, *Science*, **152**, 1619 (1966).

19 M. Fujimoto, H. D. Gesser, B. Carbutt, and A. Cohen, *Science*, **154**, 381 (1966).

20 N. Shimamoto, Y. Fujita, and T. Kwan, *Bull. Chem. Soc. Jpn.*, **43**, 580 (1970).

21 T. Katsu, M. Yanagita, and Y. Fujita, *J. Phys, Chem.*, **75**, 4064 (1971).

22 L. A. Eriksson, O. L. Malkina, V. G. Malkin, and D. R. Salahub, *J. Chem. Phys.*, **100**, 5066 (1994).

23 N. Ishii and T. Shimizu, *Chem. Phys. Lett.*, **235**, 614 (1995).

24 I. Carmichael, *J. Phys. Chem. A*, **101**, 4633 (1997).

25 S. D. Wetmor, R. J. Boyd, and L. A. Eriksson, *J. Chem. Phys.*, **106**, 7738 (1997).

26 C. B. Duke, K. L. Yip, G. P. Ceasar, A. W. Potts, and D. G. Streets, *J. Chem. Phys.*, **66**, 256 (1977); R. D. Chamber, "Fluorine in Organic Chemistry," John Wiley & Sons, New York (1973), Chap. 4, p. 64.

27 M. Shiotani, H. Kawazoe, and J. Sohma, *J. Phys. Chem.*, **88**, 413 (1982).

28 D. R. Lide eds., "CRC Handbook of Chemistry and Physics," 81st edition, CRC Press, New York (2000).